 DOI 10.1002/eji.201040719 Eur. J. Immunol. 2011. 41: 450–460

European Journal of Immunology

Molecular structure of the *Mycobacterium tuberculosis* virulence factor, mycolic acid, determines the elicited inflammatory pattern

Seppe Vander Beken[*1], *Juma'a R. Al Dulayymi*[*2], *Thomas Naessens*[1], *Gani Koza*[2], *Max Maza-Iglesias*[2], *Richard Rowles*[2], *Cornelia Theunissen*[2], *Jelle De Medts*[1], *Ellen Lanckacker*[3], *Mark S. Baird*[2] *and Johan Grooten*[1]

[1] Department of Biomedical Molecular Biology, Ghent University, Ghent, Belgium
[2] School of Chemistry, University of Wales, Bangor, UK
[3] Department of Respiratory Diseases, Ghent University Hospital, Ghent, Belgium

Mycolic acids (MAs) occur in the cell wall of *Mycobacterium tuberculosis* as variable mixtures of different classes and chain lengths. Here, we address the relationship between the structure and its inflammatory function of this virulence factor using single synthetic MA isomers, differing in oxygenation class and *cis*- versus α-methyl-*trans* proximal cyclopropane orientation. Analysis of bronchoalveolar inflammation, lung histopathology and alveolar macrophage transcription revealed a strong dependence on these meromycolic chemistries of mouse pulmonary inflammation in response to intratracheal treatments with MAs. Whereas α-MA was inert, oxygenated methoxy- and keto-MA with *cis*-cyclopropane stereochemistry elicited solid to mild inflammatory responses respectively. In *trans*-cyclopropane orientation, methoxy-MA partially lost its inflammatory activity and keto-MA exerted anti-inflammatory alternative activation of alveolar macrophages and counteracted *cis*-methoxy-MA induced airway inflammation. The differential innate immune activities of MAs demonstrated here, dependent on oxygenation class and *cis* versus α-methyl-*trans* cyclopropane chemistry, identify a novel means for *M. tuberculosis* to steer host immune responses during infection.

Keywords: Alveolar macrophage · Mycolic acid · *Mycobacterium tuberculosis* · Pulmonary inflammation

Introduction

Mycolic acids (MAs) are highly hydrophobic long-chain α-alkyl-β-hydroxy fatty acids found in the cell wall of mycolata, a bacterial taxon also including the human lung pathogen *Mycobacterium tuberculosis* [1]. These wax-like fatty acids constitute a major part of the characteristic mycobacterial cell wall architecture and, due to their hydrophobic nature, provide protection against dehydration as well as against chemical damage by host bactericidal agents and antibiotics [2]. Interestingly, whereas MAs have long been presumed to occur solely covalently bound to the arabinogalactan layer of the *M. tuberculosis* cell envelope or in the form of trehalose-bound virulence factors [3–6], Ojha and colleagues recently reported that extracellular *M. tuberculosis* bacilli may release free MAs from cell wall trehalose dimycolates to form a biofilm matrix [7, 8]. Evidence has emerged that these free MAs also have a role in the host–pathogen interaction. We previously showed that free MAs isolated from *M. tuberculosis* induce host innate airway responses characteristic of *M. tuberculosis* infection, such as pulmonary inflammation and alveolar macrophage activation and differentiation to foamy macrophages [9], a granuloma-specific cell population filled with

Correspondence: Prof. Johan Grooten
e-mail: Johan.Grooten@UGent.be

*These authors contributed equally to this work.

© 2010 WILEY-VCH Verlag GmbH & Co. KGaA, Weinheim

lipid-containing bodies within the tuberculous granulomas that surround infected macrophages [10]. Free MAs may also steer $CD4^+$ T-cell responses away from non-protective Th2-dependent immunity as indicated by the pronounced, $CD25^+$ Treg-dependent suppression of allergic airway inflammation in a mouse model of asthma following intratracheal instillation of *M. tuberculosis* MAs [11]. Additional support for a role for free MAs in the host response to infection derives from the identification of MA-reactive antibodies in blood samples from tuberculosis patients [12, 13].

MAs are chemically heterogeneous, further confounding their role in the host response to infection. In *M. tuberculosis*, three major classes – α-MA, methoxy-MA and keto-MA – are distinguished [14]. α-MA has two cyclopropane rings, which are mostly in the *cis* configuration. The oxygenated keto- and methoxy-MAs have one cyclopropane ring in either *cis* or *trans* configuration. The relative representation of these MA-classes differs considerably between different mycobacterial species and strains [15], but seems also to be directly related to virulence. Thus, the attenuated vaccine strain *M. bovis* BCG-Pasteur lacks methoxy-mycolates [16] and saprophytic mycobacteria such as *M. smegmatis* fail to produce oxygenated MAs [17]. In contrast, highly pathogenic mycobacteria such as *M. tuberculosis* [18] and *M. avium* [19] produce the oxygenated MA classes while genetic inactivation of the underlying enzymatic pathway leads to attenuation of *M. tuberculosis virulence* in mice [20]. By modifying the whole bacterial cell wall architecture, changes in relative MA composition may modify the protective function of the envelope and thereby alter the pathogenic behaviour of the respective strains. Alternatively, considering the innate immune activities elicited by chemically heterogonous MAs extracted from *M. tuberculosis* [9], it cannot be excluded that individual MA classes elicit distinct immune activities and thus differentially affect the host–pathogen interaction and pathogenicity.

To begin to address directly the intriguing question as to the specific biological function of particular MA classes, we assayed here synthetic single MA isomers of high purity and known stereochemistry as a novel tool for studying the functionality of naturally occurring chemical variations in MA-molecules. Single MA isomers, varying in *cis* versus *trans* cyclopropane configuration, and representative of the major homologues of naturally occurring α-, keto- and methoxy-MA classes were examined for their ability to elicit pulmonary inflammatory responses. The results obtained highlight the importance of both proximal and distal meromycolic functional groups in MA-mediated pulmonary inflammation and alveolar macrophage activation.

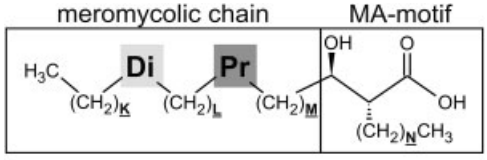
Results

Single synthetic MA isomers

The chemical identity of the single MA isomers, designed and synthesized to study the influence of MA oxygenation class and cyclopropane orientation on host pulmonary responses, is shown in Fig. 1. Thus, while keeping the proximal *cis*-cyclopropane constant, varying the distal meromycolic moiety between a cyclopropane in α-MA (*cis*-aMA), an (*S*,*S*)-α-methyl-methoxy in methoxy-MA (*cis*-mMA), and an epimerized α-methyl-ketone in keto-MA (*cis*-kMA), the role of MA oxygenation class was addressed. Furthermore, the functional relevance of stereochemical variation in proximal cyclopropane configuration within the oxygenated MA-classes was studied by also assaying the α-methyl-*trans* cyclopropane analogues: *trans*-mMA and *trans*-kMA. These variations in MA chemistry are also represented in the cell wall of *M. tuberculosis*. Furthermore, chain lengths were chosen to be identical to the most abundant *M. tuberculosis* MA-homologues [15]. An additional synthetic molecule, consisting of a mixture of four stereoisomers of the branched MA-motif and a meromycolic chain that lacks proximal and distal chemical moieties, was named the MA-backbone (MA-bb) and was included as a presumed negative control. As a reference, a natural MA-mixture, extracted from *M. tuberculosis* (*M.tb*.-MA) was also included in this study.

Pulmonary inflammation

MA was inserted into the lipid layer of phosphatidylcholine liposomes for in vivo delivery. In addition to being a macrophage targeting strategy [21], it was the intention to mimic herewith the natural situation, where MA is presented to macrophages on the surface of *M. tuberculosis* bacilli. Empty liposome treatment



Name	distal unit Di	proximal unit Pr	chain lengths K,L,M,N
cis-aMA			19,14,11,23
cis-mMA	OMe		17,16,17,23
trans-mMA	OMe		17,15,17,23
cis-kMA	O		17,18,15,23
trans-kMA	O		17,17,15,23
MA-bb	none	none	-,-,20,19

Figure 1. Chemical structure of synthetic MAs. The generic MA chemical structure, consisting of a branched MA-motif and a meromycolic chain, is depicted in the top panel. The 'Pr' and 'Di' annotations indicate respective proximal and distal meromycolic units and k, l, m, n represent numbers of carbon chain lengths. The lower panel depicts the nomenclature and chemical identity of the synthetic MA-molecules used in this study. *Cis* or *trans* refers to the *cis* or α-methyl-*trans* configuration of the proximal cyclopropane. aMA, mMA and kMA represent α-MA, methoxy-MA- and keto-MA-class isomers, respectively. MA-bb (MA-backbone) is a mixture of four stereoisomers of the MA-motif with a meromycolic chain, free of functional groups.

© 2010 WILEY-VCH Verlag GmbH & Co. KGaA, Weinheim

was then the negative carrier control used to relate the read-out parameters of the pulmonary response.

When *M.tb*.-MA was given intratracheally to C57BL/6-mice, an innate immune airway response was elicited, apparent from the significant increase in bronchoalveolar lavage (BAL) recovered cells, measured by flow cytometry, as compared to a liposome carrier treated control group (Fig. 2). The elicited inflammatory response peaked at day 2 and largely consisted of neutrophils (35.88±3.93%) and of cells from the monocytic lineage (52.51±4.48%), such as alveolar macrophages and DC (Fig. 2B). Lymphocytes (1.00±0.13%) and eosinophils (1.08±0.14%) represented only a marginal fraction of the inflammatory cell infiltrate (not shown). In absolute cell numbers, particularly neutrophils were found to be significantly enriched 2 days after instillation. This was followed by a substantial decrease in BAL neutrophil counts at day 4. Strikingly, instillation of the synthetic lipid molecule, MA-bb, representative of the MA-backbone, failed to elicit neutrophilic airway inflammation at any time point (Fig. 2B). This indicates the necessity for chemical functionality in the meromycolic chain in generating airway inflammatory responses to MAs. Indeed, the highest BAL-fluid (BALF) cell numbers and neutrophil and monocyte cell counts were found in response to the methoxy-MA isomers. Keto-MAs, although also being an oxygenated MA-class, failed to elicit this pronounced pulmonary cellular inflammation with only the *cis*-kMA variant eliciting a marginal level of inflammation. Interestingly, when comparing *cis* with methyl-*trans*-cyclopropanated variants, a greater inflammatory potency was consistently observed for both the methoxy-MAs and the keto-MAs. Finally, pulmonary cellular inflammation was not consistently observed for the non-oxygenated *cis*-aMA treated group, showing no to marginal inflammatory effects.

Histological examination of lung tissue for inflammatory pathology revealed a similar picture. Thus, 2 days after treatment with *M.tb*.-MA of natural origin and with the *cis*-mMA isomer, but not with the *trans* variant nor with the other MA-classes, some tissue inflammatory pathology was apparent, reflected by the pathology score in Fig. 3A. In those conditions where inflammatory cell infiltrates were present, the infiltrate was mostly perivascular and was never severe (Fig. 3B).

Alveolar macrophage response

To verify the response of alveolar macrophages, the prime target cells of the intratracheally administered liposomes, to the incorporated MAs, the transcriptional signature of pooled BAL-derived $CD11c^+$ cells at day 2 was quantified (Fig. 4). The $CD11c^+$ alveolar macrophage cell population was isolated by magnetic cells sorting and showed a purity of over 85% (Fig. 4A). The inflammatory mMAs induced transcription of marker genes of both classical (*Nos2*) and alternative (*Arg1*) macrophage activation (Fig. 4B). This induction was about tenfold greater for the classical macrophage activation marker *Nos2*. In line herewith, the mRNA expression levels of pro-inflammatory cytokine (*Il6* and *Il12b*) and chemokine (*Cxcl10*, *Ccl2* and *Cxcl1*) genes were upregulated upon treatment with single mMA isomers. However, none of the MAs induced expression of *Tnfa* (not shown), encoding the prominent pro-inflammatory cytokine TNF-α associated with early granuloma development [22, 23]. Interestingly, the observed difference between *cis*-mMA and *trans*-mMA in eliciting cellular inflammation was only reflected by BAL $CD11c^+$ cell expression of *Cxcl1*, which translates to the most important neutrophil chemoattracting and activating chemokine CXCL1 (also known as keratinocyte derived chemokine or KC). Typically, in parallel with the pro-inflammatory transcriptional signature, an increase in anti-inflammatory IL-10 encoding mRNA (*Il10*) was also observed upon instillation of mMAs. Instillation of the hypo-inflammatory *cis*-kMA could not upregulate alveolar macrophage activation markers, but some inflammatory activity was apparent from the induced transcription for IL-6, an acute phase inflammatory cytokine. Also an induced gene expression, although relatively small, of *Ccl2* (MCP-1) was observed using *cis*-kMA. The non-inflammatory *trans*-kMA and *cis*-aMA isomers remained inert at the host target cell transcriptional level, with the exception of *trans*-kMA. Surprisingly, this MA isomer upregulated *Arg1* threefold, whereas transcription of *Nos2* remained unchanged. Also, a nine-fold induction of *Retnla*, a second marker of alternative activated macrophages [24], was observed for this MA isomer (not shown). Thus, *trans*-kMA induces alternative macrophage activation; a status associated with anti-inflammatory and wound healing functions [25].

Inflammatory response to MA isomer mixtures

In nature, the different MA species never occur alone. α-MA molecules make up around 50% of the total MA-content of *M. tuberculosis*, whereas the abundance of the oxygenated methoxy- and keto-MA classes may vary between species, strains [15] and possibly environmental influences. Here, we verified to what extent such changes in the relative abundance of the oxygenated methoxy- and keto-MA molecules of *M. tuberculosis* may affect the inflammatory outcome. To do so, a constant amount of the hypo-inflammatory *cis*-aMA was combined with varying amounts of pro-inflammatory *cis*-mMA and non-inflammatory *trans*-kMA, thus mimicking differing ratios of oxygenated MA classes that may occur in the *M. tuberculosis* cell wall.

In a first series, addition to *cis*-aMA (12.5 μg) of increasing amounts of *cis*-mMA (12.5 μg) resulted in a dose-dependent induction of airway cellular inflammation at day 2, reflected by a 72±2% neutrophil representation in the BAL-recovered cells at the highest *cis*-mMA dose (12.5 μg) (Fig. 5A). When applying an arbitrarily set threshold value of 25% of neutrophils in the BALF for determining explicit inflammation, a dose of *cis*-mMA of as little as 5 μg was sufficient to evoke this level of pulmonary response (Fig. 5A).

In a second series, non-inflammatory *trans*-kMA was added to the *cis*-aMA and *cis*-mMA mixtures (0–12.5 μg) up to a constant total MA content of 25 μg in every sample preparation (Fig. 5B). Unlike the first series, illustrating the dose-dependent inflammatory airway response to *cis*-mMA, this second series thus was

© 2010 WILEY-VCH Verlag GmbH & Co. KGaA, Weinheim

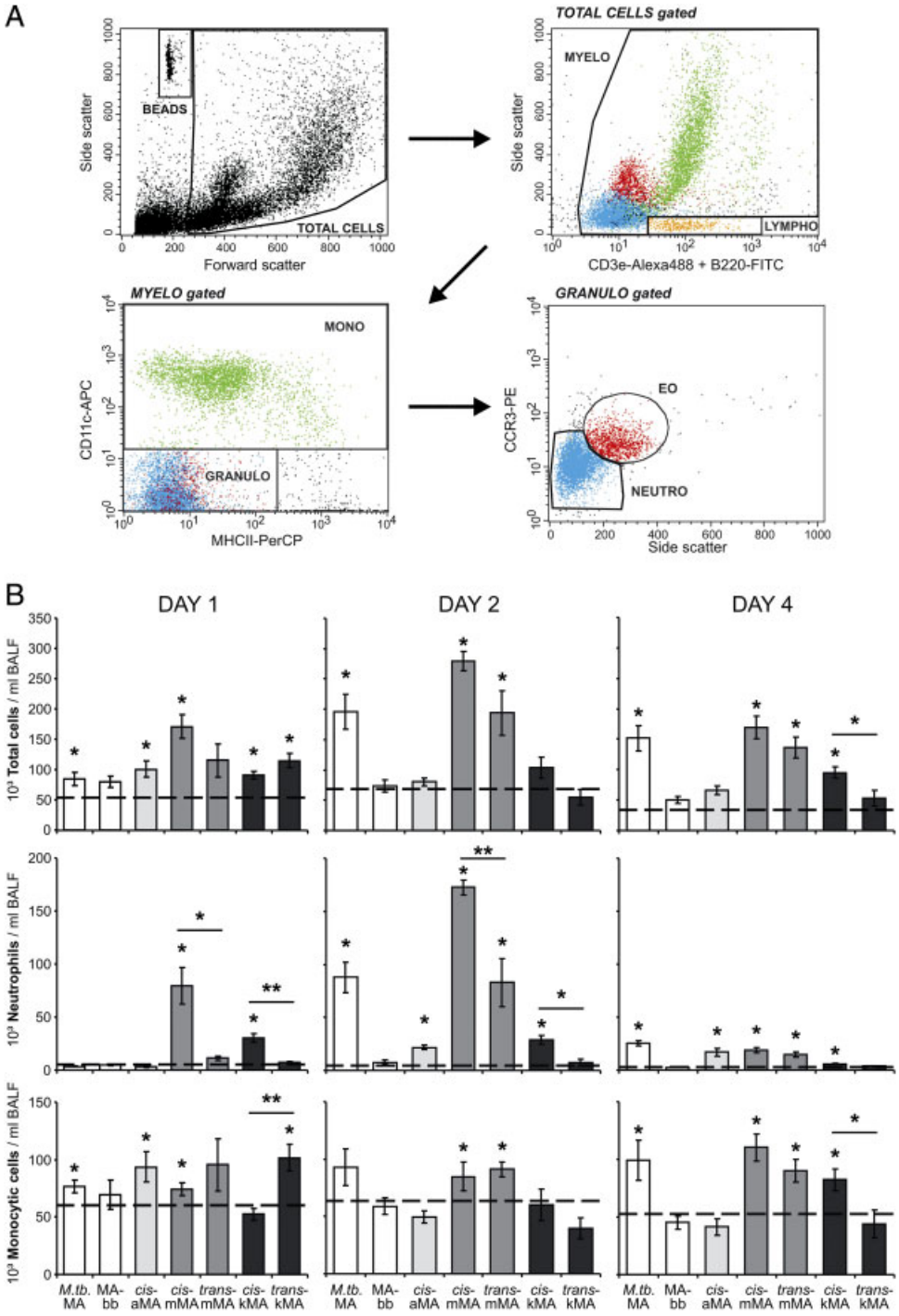


Figure 2. Bronchoalveolar inflammatory cell infiltrate. (A) Illustration of the flow cytometry analysis of BAL samples for leukocyte populations, using the method described by Van Rijt *et al.* [64], with minor modifications. Upper left panel shows the scatter profile with indication of regions for cells (total cells) and for Flow-Count beads (beads). The upper right panel dot plot was gated on the total cells scatter region and allowed for the distinction of lymphocytes (lympho) from cells of the myeloid lineage (myelo) by the expression of CD3ε (T cells) or B220 (B cells) and a low side scatter. Myelo gated cells were further subdivided into $CD11c^+$ monocytic cells (mono), which exist out of alveolar macrophages, DC and recruited monocytes, and granulocytes (granulo) that are $CD11c^-$ and have low MHC-II expression, as illustrated in the lower left panel. The distinction between eosinophils (eo) and neutrophils (neutro) from the granulo gated events was made on the basis of the CCR3-PE intensity versus side scatter dot plot regions (lower right panel). The constant amount of beads added per volume of sample allowed for calculating absolute cell numbers from the event counts within the regions. (B) Total cell numbers and counts of neutrophils and monocytic cells in BAL-samples as measured by the flow cytometry analysis on day 1, day 2 and day 4 after MA treatment. Bars show mean number per mL of BALF ± the standard error of mean ($n = 5$). Shades of grey represent the response to synthetic MA isomers belonging to the same oxygenation class. The *M.tb.*-MA as well as the MA-bb responses are shown as white bars. The broken line represents the mean cell number per mL of BALF from mice treated with carrier phosphatidylcholine liposomes alone, to which all other treatments are compared (*p<0.05 **p<0.005 by two-sided Mann–Whitney U test), unless indicated otherwise. Results are representative for two independent biological repeats.

© 2010 WILEY-VCH Verlag GmbH & Co. KGaA, Weinheim

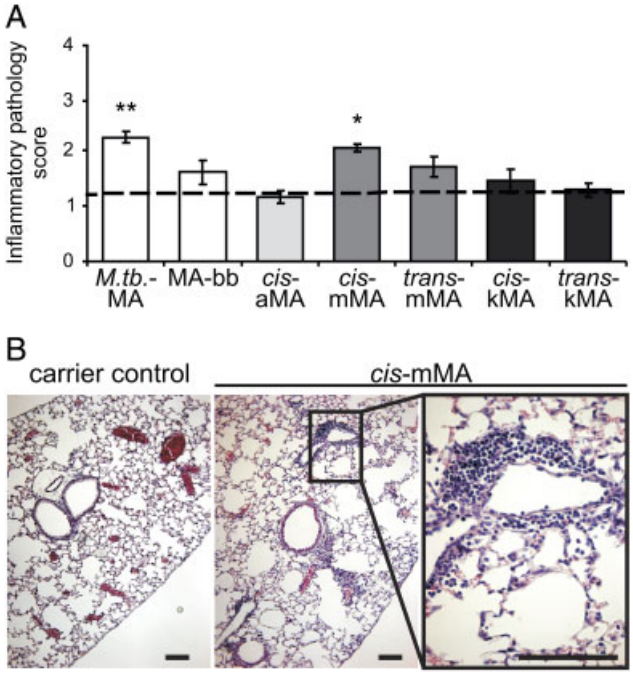


Figure 3. Lung histolopathology. Histological examination of haematoxylin and eosin-stained lavaged mouse lungs at day two after intratracheal instillation of MA carrying liposomes. (A) Shown are the mean and standard error of mean for inflammatory pathology scores ranging from 0 for no inflammatory cell infiltrates to 4 for many severe inflammatory cell infiltrates ($n = 4$). The broken line represents the mean inflammatory pathology score for lung sections of mice treated with carrier phosphatidylcholine liposomes alone, to which all other treatments are compared (*p<0.05 **p<0.005 by two-sided Mann–Whitney U test). (B) Images of stained lung sections illustrating the absence of inflammatory cell infiltrate in the carrier control group (left) as opposed to the presence of perivascular inflammatory cell infiltrates after *cis*-mMA treatment (centre). The right image is a fourfold magnification of the area indicated in the central picture. Scale bar = 100 μm.

designed to measure the inflammatory response to varying ratios of both oxygenated MAs against an equal and constant amount of non-oxygenated *cis*-aMA, conditions that may exist or be induced in *M. tuberculosis* bacilli. Strikingly, addition of *trans*-kMA resulted in a suppression of the *cis*-mMA induced neutrophilic inflammation (Fig. 5B). As an implication, the minimal amount of *cis*-mMA needed for surpassing the 25% neutrophil inflammation barrier doubled from 5 to 10 μg (Fig. 5B). This repression was reflected also at the level of $CD11c^+$ alveolar macrophage pro-inflammatory gene transcription (not shown).

Discussion

The structural study of MAs has been ongoing for more nearly a century and has documented the wide variety in the chemical structures of these molecules [14, 18, 26–34]. The relative composition of MA-classes, produced by the *M. tuberculosis* bacillus, is significantly variable between different strains and depends on the activity of enzymes involved in biosynthesis, modifications and translocation of MAs, many of which have been associated with *M. tuberculosis* infectivity, growth, survival and pathogenicity [20, 35–44]. Interestingly, expression of many of these genes changes between replicating and dormant stages of tuberculosis infection with a single strain [45]. It has recently been recognized that *M. tuberculosis* is able to produce antibiotic resistant biofilms, containing free MAs [7, 8]. We and others have published on the ability of these free MAs to induce tuberculosis infection related features in the airways such as pro-inflammatory cytokine release from macrophages and foam cell accumulation [9, 46]. The oxygenated MA-classes in particular seem to mediate most of these effects at the interface of host–pathogen interaction [46]. Yet, our understanding of the biological activity of single chemically defined MA-molecules is very limited and mostly deduced from whole organism infection and glycomycolate stimulation experiments. Here, we addressed this problem by studying the role in airway immune responses of the MA oxygenation class, defined by the distal meromycolic moiety, and the proximal cyclopropane stereochemical configuration. This was made possible because of recent advances in the chemical synthesis of single *M. tuberculosis* MAs [47–58].

The results obtained confirm that the presence and type of an oxygenated distal group in the meromycolate moiety is indeed the main determinant for at least pulmonary inflammatory potency. However, in addition they identify the proximal cyclopropane stereochemistry as a co-determinant for inflammatory potency. Thus, the presence of cyclopropanes in the meromycolic chain, as in *cis*-aMA, was on its own merely enough to elicit significant levels of pulmonary neutrophil inflammation. Considering oxygenated MA isomers, *cis*-mMA was identified as the most inflammatory MA structure. An α-methyl-*trans* orientation in the proximal cyclopropane dampened the inflammatory potency of the oxygenated isomer. A similar behaviour was observed for the second oxygenated MA class, keto-MA. While *cis*-kMA was mildly inflammatory, an α-methyl-*trans* cyclopropane in keto-MA rendered the isomer non-inflammatory. Nevertheless, this *trans*-kMA was biologically active, as indicated by its ability to suppress *cis*-mMA elicited inflammation in mix experiments.

Within the general structure–function analysis described above, specific differences between the oxygenated MA isomers could be noted at the level of the alveolar macrophage. Thus, both the *cis*-mMA and *trans*-mMA isomers elicited a comparable inflammatory transcriptional signature in these cells. Only the expression of *Cxcl1* correlated with the pro-inflammatory contribution of *cis*-cyclopropane stereochemistry in methoxy-MA on cellular inflammation. $CD11c^+$ host-cell-specific expression of *Cxcl1* could therefore be a pivotal mediator in the neutrophil recruitment to the bronchoalveolar lumen as is observed in response to MAs. For keto-MAs, the non-inflammatory feature of the *trans*-kMA isomer was accentuated at the transcriptional level by the capacity to induce a pronounced alternative activated macrophage phenotype. This most probably is at the basis of the *trans*-kMA mediated suppression of pulmonary neutrophil inflammation when the MA isomer was combined with the inflammatory *cis*-mMA in a single liposome preparation. Notably,

© 2010 WILEY-VCH Verlag GmbH & Co. KGaA, Weinheim

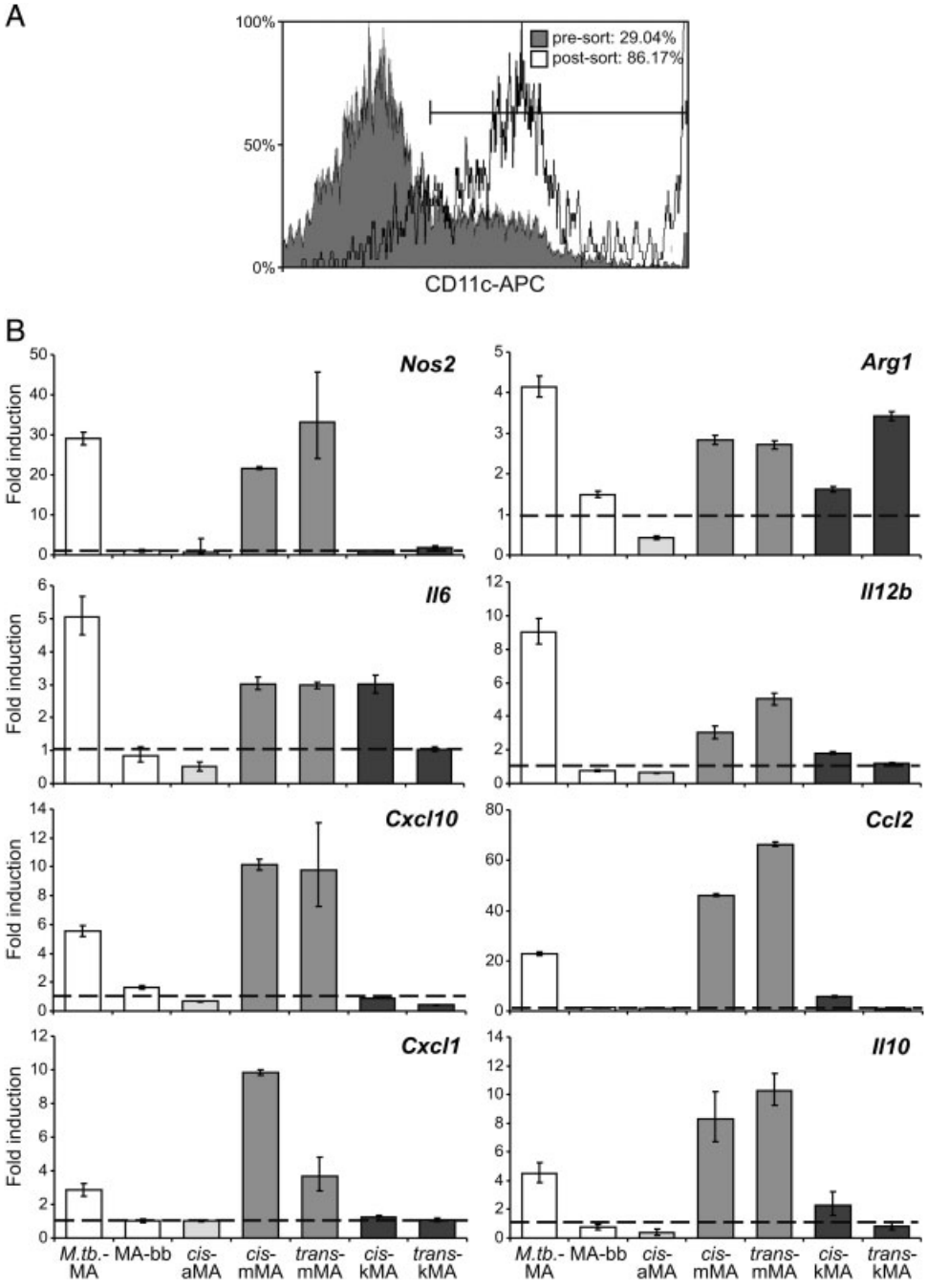


Figure 4. Alveolar macrophage activation. (A) CD11c histogram overlay of BAL cells before (grey area) and after (transparent area) magnetic cell separation. Staining with CD11c-APC revealed a consistent >85% purity. (B) Gene expression analysis by RT-qPCR was performed on the CD11c$^+$ cell fraction of the pooled BALF from MA treated mice ($n = 7$). Shown is the fold induction in expression of the macrophage activation markers *Nos2* and *Arg1*, of the pro-inflammatory genes *Il6*, *Il12b*, *Cxcl10*, *Ccl2* and *Cxcl1*, and of the anti-inflammatory cytokine encoding *Il10* in response to *M.tb.*-MA and to the single synthetic MA isomers as compared to empty liposome treatment expression levels (broken line). Expression values were normalized against mRNA abundances of the housekeeping genes *Rpl13a* and *Tbp*. Error bars represent the standard deviation on technical triplicate measurements. Results are representative for two independent biological repeats.

MAs did not elicit the expression of *Tnfa*, a key early mediator of the granuloma response to cord factor and to live *M. tuberculosis* [22, 23]. In line herewith, we never observed any granuloma-like structures in mouse lungs treated with MAs within the first 8 days of treatment.

Based on our structure–function data and the high abundance of α-MA in the *M. tuberculosis* cell wall [15], we propose that the α-MAs of *M. tuberculosis* have functions in host–pathogen interaction that are not directed at the host's innate immune response, but rather at maintaining bacillary cell wall stability and/or

© 2010 WILEY-VCH Verlag GmbH & Co. KGaA, Weinheim

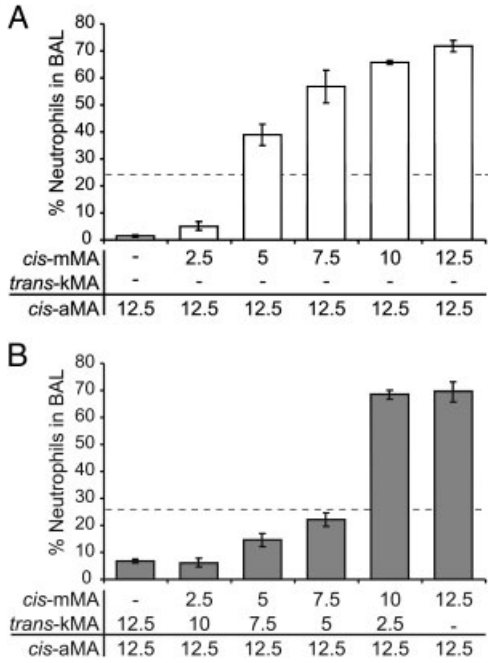


Figure 5. Inflammatory response to MA isomer mixtures. Liposome preparations containing mixtures of synthetic MA-molecules were instilled by intratracheal route and the percentile neutrophil representation in the BALF counted 48 h later. Cell counts are shown as mean ± standard error of mean of ($n = 4$). All mixtures contained 12.5 μg of *cis*-aMA as a filler. (A) Increasing amounts of the pro-inflammatory *cis*-mMA were added to the liposomes, resulting in a dose-dependent pulmonary neutrophil response. Dotted line highlights neutrophil representations of >25%, arbitrarily considered as an explicit inflammatory response. (B) The same liposome formulations as in panel A were filled up with *trans*-kMA to a constant total MA content of 25 μg.

protection against oxidative stress and xenobiotics. In contrast, it is clear from our data that the oxygenated classes exert differential regulating roles in host inflammation. In particular, methoxy-MAs were found to be inflammatory and to activate alveolar macrophage host cells. Interestingly, an isoform belonging to the second oxygenated MA-class, keto-MA, was able to suppress this, indicating that the interaction between MA molecules of different structure may define biological function. Surpassing a certain threshold in the ratio of *cis*-mMA over *trans*-mMA induced a switch from marginal to explicit pulmonary inflammation. In the context of *M. tuberculosis* infection, the ratio of the different oxygenated MAs expressed by the bacillus and exposed to the host therefore possibly co-determines the host inflammatory response. A similar hypothesis, namely that in a natural infection, *M. tuberculosis* can continually remodel its cell wall as a means of host control, was already proposed by Riley [59]. However, a direct extrapolation to virulence and pathology of the here proposed MA composition remodelling as a means of host control in pulmonary tuberculosis is difficult, because of the lack of exact figures on the relative MA composition during the natural course of infection and on the way MAs are presented to the host macrophage and to the bordering granuloma foam cells. Furthermore, unlike for cord factor [60, 61], very little is known about neither the molecular interaction partners of free MAs promoting inflammatory signalling nor the interaction of free MAs with naturally occurring lipids in the airways. In that respect, it is interesting to note that MAs have been reported to mimic and interact with cholesterol [62]. Therefore, molecular signalling pathways that involve host cell cholesterols, such as cholesterol metabolism enzymes and cholesteroid hormone receptors, may contribute to MA immune function.

Despite the difficulty to correlate them to tuberculosis infection, results presented here with free MAs show remarkably close parallels with those of studies with mutant mycobacterial strains with altered cell wall MA expression. Thus, *trans*-cyclopropanation in mycolates was shown to be important in the protective suppression of macrophage activation and a *cyclopropane–mycolic acid synthase 2* (*cmaA2*) null mutant, which lacks *trans*-cyclopropanated MAs, was hypervirulent in mice because of excessive host immune activity [42]. This observation is reflected by the weak to absent airway neutrophil recruitment and histopathology in response to the α-methyl-*trans* cyclopropanated MA isomers reported here, *trans*-mMA and *trans*-kMA, as compared to their *cis*-oriented counterparts and in particular by the anti-inflammatory capacity and the induction of alternative activation of alveolar macrophages by *trans*-kMA. On the other hand, contrary to our results with the non-inflammatory *cis*-aMA compound, a *M. tuberculosis* mutant strain, lacking the α-MA specific proximal cyclopropane synthase pcaA, lost the ability to induce pro-inflammatory macrophage activation during early infection [41]. This can be simply explained by the dramatic shift in the MA composition of the TDM preparation from the *pcaA* mutant strain in which keto-MAs became the biggest fraction. Molecules belonging to this MA class were also hypo-inflammatory to anti-inflammatory in our experiments. The anti-inflammatory action of specific oxygenated MAs such as *trans*-kMA may also explain the apparent inhibition of macrophage IL-12p40 by mycolates generated by *hma* (*mmaA4*), which encodes a methyl transferase required for introducing the distal oxygen containing modifications of MAs [37]. The mycolate products of other genes – including *mmaA2* and *KasB* – involved in MA biosynthesis and associated with *M. tuberculosis* in vivo virulence and/or growth [38, 39] remain to be characterized for their impact on MA composition and its correlation with specific host immune functions.

Considerable more structural variation exists within the *M. tuberculosis* MA pool than was presented in the scope of this study. In addition to the oxygenation level and proximal cyclopropane configuration studied here, future research should also determine biological functions of other MA chemical characteristics such as chain lengths, double bonds and glycosylations. The latter can now be addressed for trehalose containing synthetic mycolates of unique single structure because it has recently become possible to chemically prepare these cord factors [63]. The current approach, using synthetic MA isomers and derivatives based on major components in the cell wall of *M. tuberculosis*, allows for such rationalized screening. Furthermore, synthetic MAs represent useful tools for mechanistic studies from which we can learn how this successful human pathogen regulates inflammation

© 2010 WILEY-VCH Verlag GmbH & Co. KGaA, Weinheim

and host immune responses, and exploit these mechanisms for biomedical applications. In particular, the anti-inflammatory feature of *trans*-kMA might be of significance in therapeutics of inflammatory disorders while the milder pathological profile of (oxygenated) MAs as compared to cord factors might prove them better suited for use in adjuvant preparations.

Materials and methods

Animals

Female C57BL/6J mice (Janvier, Le-Genest-Saint-Isle, France) were housed under specific pathogen free conditions in individually ventilated cages. Mice were 8–12 wk old at the start of experiments.

MAs

The natural MA reference used was extracted from *M. tuberculosis* H37Rv (*M.tb*.-MA) and purchased from Sigma (St. Louis, MO, USA). The synthesis of the chemically defined synthetic MA isomers has been described before [47–58]. The α-methyl-*trans* methoxy-MA (*trans*-mMA) was prepared by a variation of the methods described for the keto-MA variant *trans*-kMA [56]. Briefly, a single (*R,R*)-stereoisomer at the hydroxyl acid group was prepared using a Frater-type alkylation of a R-3-hydroxy-acid. The absolute stereochemistries of *cis*-cyclopropane and α-methyl-*trans*-cyclopropane units were defined by starting from an enzyme-induced desymmetrization of *cis*-cyclopropane-1,2-diol or a derivative, or by asymmetric cyclopropanation of alkenes derived from mannitol or dihydroascorbic acid. The methoxymethyl subunit of the methoxy-MAs and the α-methyl-keto group of the keto-MAs were introduced in a stereocontolled manner by ring opening of a chiral epoxide. A model synthetic compound, referred to as MA-backbone (MA-bb), containing the MA-motif as a mixture of stereoisomers and a meromycolic chain free of functional moieties, was obtained by condensation of two methyl behenate molecules with sodium methoxide, followed by reduction of the derived methyl ester of the corresponding keto-acid and ester hydrolysis. Purity and structural validation of the synthetic MAs were obtained by MALDI mass spectrometry, by proton and carbon NMR at 500 and 125 MHz, and by thin layer chromatography with a solvent system consisting of 10:1 petrol:ether followed by phosphomolybdic acid visualization.

Preparation and administration of MA carrying liposomes

All MAs were incorporated into liposomes as described earlier [9]. Briefly, the compounds were mixed with phosphatidylcholine (Sigma) in chloroform. The chloroform was evaporated and the lipids recovered in PBS (Lonza, Walkersville, MD, USA). After sonication and vortexing, samples of 25 μg MA/100 μL/mouse were administered intratracheally, unless indicated otherwise. An empty liposome control was prepared similarly, but without the addition of any MA-compound. Liposome formulations were free of endotoxin as determined by a chromogenic *Limulus* amebocyte lysate assay (Genscript, Piscataway, NJ, USA).

Pulmonary inflammation read-out

Mice ($n = 5$ per experimental group) were sacrificed 48 h after intratracheal instillation to assess inflammatory parameters. Hereto, a BAL with Ca^{2+}- and Mg^{2+}-free Hank's buffered salt solution (Gibco-Invitrogen, Paisley, Scotland, UK), supplemented with 0.05 mM EDTA, was performed. BAL extruded cell counts and cell type composition was analyzed by flow cytometry (BD FACSCalibur, BD Biosciences, Franklin Lakes, NJ, USA) as previously described [64], with minor modifications. Cells, pre-incubated with Fc-block (BD Pharmingen), were classified as monocytes (alveolar macrophages and elicited monocytes and DC), neutrophils, eosinophils or lymphocytes based on forward and side scatter gating and fluorescence intensities for Alexa488-labelled anti-CD3e (BD Pharmingen), FITC-labelled anti-B220 (BD Pharmingen), PE-labelled anti-CCR3 (R&D Systems, Minneapolis, MN, USA), allophycocyanin-labelled anti-CD11c (BD Pharmingen) antibodies and streptavidin-PerCP (BD Pharmingen) recognizing biotin labelled anti-I-A^b (BD Pharmingen). Additionally, the total number of BAL retrieved cells was calculated from the measured total cell count relative to the number of Flow-Count beads (Beckman Coulter, Brea, CA, USA) of which a constant amount was added to the sample. The differential cell counts were confirmed by morphological examination of the BAL extruded cells on cytospin preparations stained with May-Grünwald/Giemsa. Lavaged lungs were fixed with a 4% paraformaldehyde solution, dehydrated in ethanol and embedded into paraffin, using a Shandon Citadel 2000 tissue processor (Thermo Scientific).

Lung histopathology

For lung histological examination, paraffin embedded tissue from 2 days after MA treatment was cut into 4-μm thin slices using a microtome (Microm HM36O, Thermo Scientific) and stained with eosin and haematoxylin (Shandon Varistain 24–4, Thermo Scientific). Inflammation was scored by a skilled pathologist in a blinded sample set-up. Scores from 0 to 4 were given for four lungs per experimental group according to the amount and severity of peribronchial and perivascular inflammatory cell infiltrates.

Alveolar macrophage transcription

The $CD11c^+$ BAL cell fraction was separated from pooled samples by magnetic sorting with biotin anti-mouse CD11c (BD Pharmin-

© 2010 WILEY-VCH Verlag GmbH & Co. KGaA, Weinheim

Table 1. Primer sequences used for reverse transcriptase–quantitative PCR of mouse gene expression

Gene	GenBank Accession	Primer	Sequence (5′→3′)	Length (nt)
Nos2	NM_010927	forward	GGAGCAGGTGGAAGACTATTTCTT	24
		reverse	CATGATAACGTTTCTGGCTCTTGA	24
Arg1	NM_007482	forward	TGAACACGGCAGTGGCTTTA	20
		reverse	GCATTCACAGTCACTTAGGTGGTTTA	26
Il6	NM_031168	forward	TAGTCCTTCCTACCCCAATTTCC	23
		reverse	TTGGTCCTTAGCCACTCCTTC	21
Il12b	NM_008352	forward	AACCAGGGCCTTCTTTAG	18
		reverse	GATCTGCCTGCCTTGGTCT	19
Cxcl10	NM_021274	forward	GTCACATCAGCTGCTACTC	19
		reverse	GTGGTTAAGTTCGTGCTTAC	20
Ccl2	NM_011333	forward	GCATCTGCCCTAAGGTCTTCA	21
		reverse	TGCTTGAGGTGGTTGTGGAA	20
Cxcl1	NM_008176	forward	ACCCGCTCGCTTCTCTGTG	19
		reverse	AGCCTCGCGACCATTCTTG	19
Il10	NM_010548	forward	GGTGTCCTTTCAATTGCTCTCAT	23
		reverse	TCACAACTCTCTTAGGAGCTCTGAACT	27
Rpl13a[a)]	NM_009438	forward	CCTGCTGCTCTCAAGGTTGTT	21
		reverse	TGGCTGTCACTGCCTGGTACTT	22
Tbp[a)]	NM_013684	forward	TCTACCGTGAATCTTGGCTGTAAA	24
		reverse	TTCTCATGATGACTGCAGCAAA	22

[a)] Housekeeping genes for sample normalization.

gen) coated Dynal magnetic beads (CELLection Biotin Binder Kit, Invitrogen). Total RNA was isolated (Total Aurum RNA mini-kit, Bio-Rad Laboratories, Hercules, CA, USA) for subsequent reverse transcriptase-quantitative PCR (LightCycler 480, Roche) analysis. Invitrogen provided the primers listed in Table 1, designed using DNAStar (Madison, WI, USA) software.

Statistical analysis

Statistics were performed using SPSS 15.0 (IBM, Chicago, IL, USA) and GraphPad Prism 5 (GraphPad Software, La Jolla, CA, USA) software. Following outlier statistics in order to choose between performing a one-way ANOVA or Kruskal–Wallis nonparametric test, Gaussian distribution of response parameters was checked using a Kolmogorov–Smirnov test. Equal variance testing was ignored because of comparable sample sizes. Differences in mean between each two independent experimental groups were analyzed using an unpaired *t*-test or the non-parametrical Mann–Whitney *U* test at 95% confidence interval. No statistical analysis was done for gene expression data, as this concerned data of pooled samples.

Acknowledgements: This work was supported by the Wellcome Trust (085656/Z/08/Z); Asthma UK (08/053); and Research Foundation-Flanders (G.0376.05N; G.0063.09N). Additional financial support to J. G. and S. V. B. was provided by the IAP6/18, funded by the Interuniversity Attraction Poles Program and initiated by the Belgian State Science Policy Office. R. R. thanks the EPSRC for the award of a PhD studentship. The authors thank Samuel Noppen for excellent technical support.

Conflict of interest: The authors declare no financial or commercial conflict of interest.

References

1 **Daffe, M., Laneelle, M. A., Asselineau, C., Levyfrebault, V. and David, H.,** Taxonomic value of Mycobacterial fatty-acids: proposal for a method of analysis. *Ann. Microbiol.* 1983. **B134**: 241–256.

2 **Kremer, L. S. and Besra, G. S.,** Current status and future development of antitubercular chemotherapy. *Expert Opin. Investig. Drugs* 2002. **11**: 1033–1049.

3 **Brennan, P. J.,** Structure, function, and biogenesis of the cell wall of *Mycobacterium tuberculosis*. *Tuberculosis* 2003. **83**: 91–97.

4 **Hunter, R. L., Olsen, M. R., Jagannath, C. and Actor, J. K.,** Multiple roles of cord factor in the pathogenesis of primary, secondary, and cavitary tuberculosis, including a revised description of the pathology of secondary disease. *Ann. Clin. Lab. Sci.* 2006. **36**: 371–386.

5 **Karakousis, P. C., Bishai, W. R. and Dorman, S. E.,** *Mycobacterium tuberculosis* cell envelope lipids and the host immune response. *Cell. Microbiol.* 2004. **6**: 105–116.

6 **Ryll, R., Kumazawa, Y. and Yano, I.,** Immunological properties of trehalose dimycolate (cord factor) and other mycolic acid-containing glycolipids – a review. *Microbiol. Immunol.* 2001. **45**: 801–811.

© 2010 WILEY-VCH Verlag GmbH & Co. KGaA, Weinheim

7 **Ojha, A. K., Baughn, A. D., Sambandan, D., Hsu, T., Trivelli, X., Guerardel, Y., Alahari, A. *et al.*,** Growth of *Mycobacterium tuberculosis* biofilms containing free mycolic acids and harbouring drug-tolerant bacteria. *Mol. Microbiol.* 2008. **69**: 164–174.

8 **Ojha, A. K., Trivelli, X., Guerardel, Y., Kremer, L. and Hatfull, G.,** Enzymatic hydrolysis of trehalose dimycolate releases free mycolic acid during mycobacterial growth in biofilms. *J. Biol. Chem.* 2010. **285**: 17380–17389.

9 **Korf, J., Stoltz, A., Verschoor, J., De Baetselier, P. and Grooten, J.,** The *Mycobacterium tuberculosis* cell wall component mycolic acid elicits pathogen-associated host innate immune responses. *Eur. J. Immunol.* 2005. **35**: 890–900.

10 **Russell, D. G., Cardona, P. J., Kim, M. J., Allain, S. and Altare, F.,** Foamy macrophages and the progression of the human tuberculosis granuloma. *Nat. Immunol.* 2009. **10**: 943–948.

11 **Korf, J. E., Pynaert, G., Tournoy, K., Boonefaes, T., Van Oosterhout, A., Ginneberge, D., Haegeman, A. *et al.*,** Macrophage reprogramming by mycolic acid promotes a tolerogenic response in experimental asthma. *Am. J. Respir. Crit. Care Med.* 2006. **174**: 152–160.

12 **Pan, J., Fujiwara, N., Oka, S., Maekura, R., Ogura, T. and Yano, I.,** Anti-cord factor (trehalose 6,6'dimycolate) IgG antibody in tuberculosis patients recognizes mycolic acid subclasses. *Microbiol. Immunol.* 1999. **43**: 863–869.

13 **Schleicher, G. K., Feldman, C., Vermaak, Y. and Verschoor, J. A.,** Prevalence of anti-mycolic acid antibodies in patients with pulmonary tuberculosis co-infected with HIV. *Clin. Chem. Lab. Med.* 2002. **40**: 882–887.

14 **Watanabe, M., Aoyagi, Y., Mitome, H., Fujita, T., Naoki, H., Ridell, M. and Minnikin, D. E.,** Location of functional groups in mycobacterial meromycolate chains; the recognition of new structural principles in mycolic acids. *Microbiology* 2002. **148**: 1881–1902.

15 **Watanabe, M., Aoyagi, Y., Ridell, M. and Minnikin, D. E.,** Separation and characterization of individual mycolic acids in representative mycobacteria. *Microbiology (Reading, England)* 2001. **147**: 1825–1837.

16 **Minnikin, D. E., Parlett, J. H., Magnusson, M., Ridell, M. and Lind, A.,** Mycolic acid patterns of representatives of Mycobacterium-Bovis Bcg. *J. Gen. Microbiol.* 1984. **130**: 2733–2736.

17 **Wong, M. Y. H., Steck, P. A. and Gray, G. R.,** Major mycolic acids of Mycobacterium-Smegmatis – characterization of their homologous series. *J. Biol. Chem.* 1979. **254**: 5734–5740.

18 **Minnikin, D. E. and Polgar, N.,** Methoxymycolic and ketomycolic acids from human Tubercle Bacilli. *Chem. Commun.* 1967. **22**: 1172–1174.

19 **Levyfrebault, V., Goh, K. S. and David, H. L.,** Mycolic acid analysis for clinical-identification of Mycobacterium-Avium and related Mycobacteria. *J. Clin. Microbiol.* 1986. **24**: 835–839.

20 **Dubnau, E., Chan, J., Raynaud, C., Mohan, V. P., Laneelle, M. A., Yu, K. M., Quemard, A. *et al.*,** Oxygenated mycolic acids are necessary for virulence of *Mycobacterium tuberculosis* in mice. *Mol. Microbiol.* 2000. **36**: 630–637.

21 **Vyas, S. P. and Khatri, K.,** Liposome-based drug delivery to alveolar macrophages. *Expert Opin. Drug Deliv.* 2007. **4**: 95–99.

22 **Hernandez-Pando, R., Orozco, H., Arriaga, K., Sampieri, A., Larriva-Sahd, J. and Madrid-Marina, V.,** Analysis of the local kinetics and localization of interleukin-1 alpha, tumour necrosis factor-alpha and transforming growth factor-beta, during the course of experimental pulmonary tuberculosis. *Immunology* 1997. **90**: 607–617.

23 **Welsh, K. J., Abbott, A. N., Hwang, S. A., Indrigo, J., Armitige, L. Y., Blackburn, M. R., Hunter, R. L., Jr., and Actor, J. K.,** A role for tumour necrosis factor-alpha, complement C5 and interleukin-6 in the initiation and development of the mycobacterial cord factor trehalose 6,6'-dimycolate induced granulomatous response. *Microbiology (Reading, England)* 2008. **154**: 1813–1824.

24 **Raes, G., Brys, L., Dahal, B. K., Brandt, J., Grooten, J., Brombacher, F., Vanham, G. *et al.*,** Macrophage galactose-type C-type lectins as novel markers for alternatively activated macrophages elicited by parasitic infections and allergic airway inflammation. *J. Leukoc. Biol.* 2005. **77**: 321–327.

25 **Martinez, F. O., Helming, L. and Gordon, S.,** Alternative activation of macrophages: An immunologic functional perspective. *Annu. Rev. Immunol.* 2009. **27**: 451–483.

26 **Asseline, C., Tocanne, G. and Tocanne, J. F.,** Stereochemistry of mycolic acids. *Bull. Soc. Chim. France* 1970. **4**: 1445–1449.

27 **Minnikin, D. E., Kremer, L., Dover, L. G. and Besra, G. S.,** The methyl-branched fortifications of *Mycobacterium tuberculosis*. *Chem. Biol.* 2002. **9**: 545–553.

28 **Minnikin, D. E., Kusamran, K. and Polgar, N.,** Structure and distribution of mycolic acids of Mycobacteria. *J. Gen. Microbiol.* 1971. **68**: iii–iv.

29 **Minnikin, D. E. and Minnikin, S. M.,** Nuclear magnetic-resonance studies on the mycolic acids. *J. Am. Oil Chem. Soc.* 1980. **57**: A163-A163.

30 **Minnikin, D. E. and Polgar, N.,** Studies on the mycolic acids from human tubercle bacilli. *Tetrahedron Lett.* 1966. **23**: 2643–2647.

31 **Minnikin, D. E. and Polgar, N.,** Stereochemical studies on mycolic acids. *Chem. Commun.* 1966. **18**: 648–649.

32 **Minnikin, D. E. and Polgar, N.,** Mycolic Acids from Human and Avian Tubercle Bacilli. *Chem. Commun.* 1967. **18**: 916–918.

33 **Minnikin, D. E. and Polgar, N.,** Structural Studies on Mycolic Acids. *Chem. Commun.* 1967. **7**: 312–314.

34 **Villeneuve, M., Kawai, M., Kanashima, H., Watanabe, M., Minnikin, D. E. and Nakahara, H.,** Temperature dependence of the Langmuir monolayer packing of mycolic acids from *Mycobacterium tuberculosis*. *Biochim. Biophys. Acta* 2005. **1715**: 71–80.

35 **Barkan, D., Liu, Z., Sacchettini, J. C. and Glickman, M. S.,** Mycolic acid cyclopropanation is essential for viability, drug resistance, and cell wall integrity of *Mycobacterium tuberculosis*. *Chem. Biol.* 2009. **16**: 499–509.

36 **Bhatt, A., Fujiwara, N., Bhatt, K., Gurcha, S. S., Kremer, L., Chen, B., Chan, J. *et al.*,** Deletion of kasB in *Mycobacterium tuberculosis* causes loss of acid-fastness and subclinical latent tuberculosis in immunocompetent mice. *Proc. Natl. Acad. Sci. USA* 2007. **104**: 5157–5162.

37 **Dao, D. N., Sweeney, K., Hsu, T., Gurcha, S. S., Nascimento, I. P., Roshevsky, D., Besra, G. S. *et al.*,** Mycolic acid modification by the mmaA4 gene of *M. tuberculosis* modulates IL-12 production. *Plos Pathog.* 2008. **4**: e1000081.

38 **Gao, L. Y., Laval, F., Lawson, E. H., Groger, R. K., Woodruff, A., Morisaki, J. H., Cox, J. S. *et al.*,** Requirement for kasB in Mycobacterium mycolic acid biosynthesis, cell wall impermeability and intracellular survival: implications for therapy. *Mol. Microbiol.* 2003. **49**: 1547–1563.

39 **Glickman, M. S.,** The mmaA2 gene of *Mycobacterium tuberculosis* encodes the distal cyclopropane synthase of the alpha-mycolic acid. *J. Biol. Chem.* 2003. **278**: 7844–7849.

40 **Glickman, M. S., Cox, J. S. and Jacobs, W. R.,** A novel mycolic acid cyclopropane synthetase is required for cording, persistence, and virulence of *Mycobacterium tuberculosis*. *Mol. Cell* 2000. **5**: 717–727.

41 **Rao, V., Fujiwara, N., Porcelli, S. A. and Glickman, M. S.,** *Mycobacterium tuberculosis* controls host innate immune activation through cyclopropane modification of a glycolipid effector molecule. *J. Exp. Med.* 2005. **201**: 535–543.

© 2010 WILEY-VCH Verlag GmbH & Co. KGaA, Weinheim

42 **Rao, V., Gao, F., Chen, B., Jacobs, W. R., Jr., and Glickman, M. S.,** Trans-cyclopropanation of mycolic acids on trehalose dimycolate suppresses *Mycobacterium tuberculosis*-induced inflammation and virulence. *J. Clin. Invest.* 2006. **116**: 1660–1667.

43 **Takayama, K., Wang, C. and Besra, G. S.,** Pathway to synthesis and processing of mycolic acids in *Mycobacterium tuberculosis*. *Clin. Microbiol. Rev.* 2005. **18**: 81–101.

44 **Yuan, Y., Zhu, Y., Crane, D. D. and Barry, C. E., 3rd.,** The effect of oxygenated mycolic acid composition on cell wall function and macrophage growth in *Mycobacterium tuberculosis*. *Mol. Microbiol.* 1998. **29**: 1449–1458.

45 **Boshoff, H. I. and Barry Iii, C. E.,** Is the mycobacterial cell wall a hopeless drug target for latent tuberculosis? *Drug Discov. Today Dis. Mech.* 2006. **3**: 237–245.

46 **Peyron, P., Vaubourgeix, J., Poquet, Y., Levillain, F., Botanch, C., Bardou, F., Daffe, M. *et al.*,** Foamy macrophages from tuberculous patients' granulomas constitute a nutrient-rich reservoir for *M. tuberculosis* persistence. *PLoS Pathog.* 2008. **4**: e1000204.

47 **Al Dulayymi, J. R., Baird, M. S. and Roberts, E.,** The synthesis of single enantiomers of a meromycolic acid. *Tetrahedron Lett.* 2000. **41**: 7107–7110.

48 **Al Dulayymi, J. R., Baird, M. S. and Roberts, E.,** The synthesis of a single enantiomer of a major alpha-mycolic acid of *Mycobacterium tuberculosis*. *Chem. Commun.* 2003. 228–229.

49 **Al Dulayymi, J. R., Baird, M. S. and Roberts, E.,** The synthesis of a single enantiomer of a major alpha-mycolic acid of M-tuberculosis. *Tetrahedron* 2005. **61**: 11939–11951.

50 **Al Dulayymi, J. R., Baird, M. S., Roberts, E., Deysel, M. and Verschoor, J.,** The first syntheses of single enantiomers of the major methoxymycolic acid of *Mycobacterium tuberculosis*. *Tetrahedron* 2007. **63**: 2571–2592.

51 **Al Dulayymi, J. R., Baird, M. S., Roberts, E. and Minnikin, D. E.,** The synthesis of single enantiomers of meromycolic acids from mycobacterial wax esters. *Tetrahedron* 2006. **62**: 11867–11880.

52 **Al Dulayymi, A. R., Al Dulayymi, J. R., Baird, M. S. and Koza, G.,** Simple 4-carbon and 5-carbon cyclopropane derivatives as synthons. *Zhurnal Organicheskoi Khimii* 1997. **33**: 867–885.

53 **Al-Dulayymi, J. R., Baird, M. S., Mohammed, H., Roberts, E. and Clegg, W.,** The synthesis of one enantiomer of the alpha-methyl-trans-cyclopropane unit of mycolic acids. *Tetrahedron* 2006. **62**: 4851–4862.

54 **Coxon, G. D., Al Dulayymi, J. R., Morehouse, C., Brennan, P. J., Besra, G. S., Baird, M. S. and Minnikin, D. E.,** Synthesis and properties of methyl 5-(1 ' R,2 ' S)-(2-octadecylcycloprop-1-yl)pentanoate and other omega-19 chiral cyclopropane fatty acids and esters related to mycobacterial mycolic acids. *Chem. Phys. Lipids* 2004. **127**: 35–46.

55 **Coxon, G. D., Knobl, S., Roberts, E., Baird, M. S., Al Dulayymi, J. R., Besra, G. S., Brennan, P. J. and Minnikin, D. E.,** The synthesis of both enantiomers of lactobacillic acid and mycolic acid analogues. *Tetrahedron Lett.* 1999. **40**: 6689–6692.

56 **Koza, G. and Baird, M. S.,** The first synthesis of single enantiomers of ketomycolic acids. *Tetrahedron Lett.* 2007. **48**: 2165–2169.

57 **Koza, G., Rowles, R., Theunissen, C., Al-Dulayymi, J. R. and Baird, M. S.,** The synthesis of single enantiomers of trans-alkene-containing mycolic acids. *Tetrahedron Lett.* 2009. **50**: 7259–7262.

58 **Koza, G., Theunissen, C., Al Dulayymi, J. R. and Baird, M. S.,** The synthesis of single enantiomers of mycobacterial ketomycolic acids containing cis-cyclopropanes. *Tetrahedron* 2009. **65**: 10214–10229.

59 **Riley, L. W.,** Of mice, men, and elephants: *Mycobacterium tuberculosis* cell envelope lipids and pathogenesis. *J. Clin. Invest.* 2006. **116**: 1475–1478.

60 **Hunter, R. L., Olsen, M., Jagannath, C. and Actor, J. K.,** Trehalose 6,6'-dimycolate and lipid in the pathogenesis of caseating granulomas of tuberculosis in mice. *Am. J. Pathol.* 2006. **168**: 1249–1261.

61 **Schoenen, H., Bodendorfer, B., Hitchens, K., Manzanero, S., Werninghaus, K., Nimmerjahn, F., Agger, E. M. *et al.*,** Cutting edge: Mincle is essential for recognition and adjuvanticity of the mycobacterial cord factor and its synthetic analog trehalose-dibehenate. *J. Immunol.* **184**: 2756–2760.

62 **Benadie, Y., Deysel, M., Siko, D. G., Roberts, V. V., Van Wyngaardt, S., Thanyani, S. T., Sekanka, G. *et al.*,** Cholesteroid nature of free mycolic acids from *M. tuberculosis*. *Chemistry Phys. Lipids* 2008. **152**: 95–103.

63 **Al Dulayymi, J. R., Baird, M. S., Maza-Iglesias, M., Vander Beken, S. and Grooten, J.,** The first unique synthetic mycobacterial cord factors. *Tetrahedron Lett.* 2009. **50**: 3702–3705.

64 **van Rijt, L. S., Kuipers, H., Vos, N., Hijdra, D., Hoogsteden, H. C. and Lambrecht, B. N.,** A rapid flow cytometric method for determining the cellular composition of bronchoalveolar lavage fluid cells in mouse models of asthma. *J. Immunol. Methods* 2004. **288**: 111–121.

Abbreviations: **BAL:** bronchoalveolar lavage · **MA:** mycolic acid

Full correspondence: Prof. Johan Grooten, Lab Molecular Immunology, Department of Biomedical Molecular Biology–Faculty of Sciences, Ghent University, Technologiepark 927, B-9052 Ghent (Zwijnaarde), Belgium
Fax: +32-9-3313609
e-mail: Johan.Grooten@UGent.be

Received: 8/6/2010
Revised: 20/10/2010
Accepted: 17/11/2010
Accepted article online: 8/12/2010

© 2010 WILEY-VCH Verlag GmbH & Co. KGaA, Weinheim